Porphyrin-linked nitroimidazole antibiotics targeting *Porphyromonas gingivalis*†

Benjamin C.-M. Yap,[a] Grace L. Simpkins,[a] Charles A. Collyer,[b] Neil Hunter[c] and Maxwell J. Crossley*[a]

Received 3rd March 2009, Accepted 29th April 2009
First published as an Advance Article on the web 27th May 2009
DOI: 10.1039/b904340c

Periodontal disease is an inflammatory process affecting supporting tissues surrounding the teeth. The anaerobic Gram-negative bacterium *Porphyromonas gingivalis* is implicated in the disease. This organism requires the uptake of porphyrins most apparently as haem **1** from local haemorrhage and it has a HA2 receptor on the outer membrane for this purpose that provides the opportunity to achieve selective anti-microbial activity. Uniquely, this receptor is based on recognition of porphyrin macrocycle and on a propionic acid side-chain rather than recognition of the coordinated metal ion through chelation, a process used by other organisms with the HasA porphyrin receptor. Porphyrin–antibiotic conjugates **11**, **12**, **13a** and **13b** were designed as potential highly selective *P. gingivalis* inhibitors, a key point being that they are based on the use of free-base porphyrins to render them unpalatable to other organisms. These compounds were synthesised from metronidazole **4** and deuteroporphyrin IX **3**. Conjugates **11**, **12**, **13a** and **13b** are all recognised by the HA2 receptor of *P. gingivalis*, bind as strongly as haem **1** to HA2 and are highly effective. For example, the amide-linked mono-metronidazole mono-acid adducts **11** and **12** have the same growth inhibitory activity towards *P. gingivalis* and both are two-fold more active than metronidazole **4** and ten- to twenty-fold more effective than the metronidazole derivative, amine **5**. The methyl esters **9** and **10**, in contrast, are not recognised by HA2 and are ineffective in inhibiting *P. gingivalis*, leading to the conclusion that capture by HA2 may be necessary for activity of the adducts. Preliminary growth inhibition assays involving a range of bacteria have demonstrated the high selectivity of conjugates **13a** and **13b** towards *P. gingivalis*.

Introduction

The black-pigmented Gram-negative bacterium *Porphyromonas gingivalis*, a key etiological agent of periodontal disease, is a porphyrin auxotroph.[1] The absolute requirement for exogenous porphyrin, as a growth factor, is satisfied by haem **1**, usually as haemin **2** (Hm) (a chloride salt of the iron-oxidized form of haem **1**) or as haemoglobin (Hb).[1–3] The active transport of captured haem and iron-loaded siderophores across the outer membrane (OM) into the periplasmic space involves energy-transducing TonB proteins. Hence, the OM receptors are often referred to as TonB-dependent receptors.[2,4]

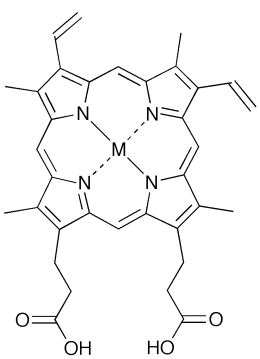

1 M = Fe(II)
2 M = Fe(III)Cl

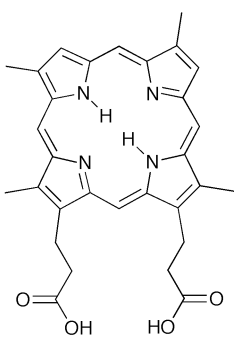

3

Metronidazole **4**, a nitroimidazole antibiotic, is a current treatment for periodontal disease and it exhibits excellent activity but it is also active against a broad range of anaerobic bacteria.[5,6] The broad spectrum of bacterial activity provides impetus for the formulation of a selective inhibitor of *P. gingivalis*, perhaps exploiting the porphyrin transport mechanism. This would overcome indiscriminate suppression of anaerobic bacteria, including species that are potentially beneficial, within this polymicrobial ecosystem.[7]

[a]*School of Chemistry, The University of Sydney, NSW 2006, Australia. E-mail: m.crossley@chem.usyd.edu.au; Fax: +61 2 93513329; Tel: +61 2 93512751*
[b]*School of Molecular and Microbial Biosciences, The University of Sydney, NSW 2006, Australia*
[c]*Institute of Dental Research, Westmead Millennium Institute and Centre for Oral Health, Westmead, NSW 2145, Australia*

† Electronic supplementary information (ESI) available: Fig. S1: structures of **9** and **10** with numbering. Fig. S2: 2D ^{1}H NMR COSY of **10**. Fig. S3: expansion of 2D ^{1}H NMR COSY of **10**. Fig. S4: 2D ^{1}H NMR NOESY of **10**. Fig. S5: expansion of 2D ^{1}H NMR NOESY of **10**. Fig. S6: expansion of 2D ^{1}H NMR NOESY of **9**. Table S7: chemical shifts, coupling and assignment of peaks for **9** from NOESY spectrum. Table S8: chemical shifts, coupling and assignment of peaks for **10** from NOESY spectrum. See DOI: 10.1039/b904340c

This journal is © The Royal Society of Chemistry 2009

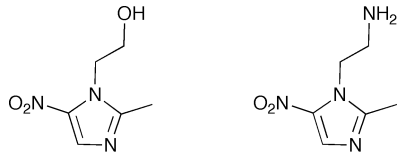

4 **5**

Porphyrins and metalloporphyrins have been used as therapeutic agents for many years and their significance is rapidly rising. For instance, gallium protoporphyrin has potent inhibitory activity against a range of bacterial species.[8]

This work involves the design, synthesis and evaluation of porphyrin–metronidazole conjugates, the amide-linked mono-metronidazole mono-acid adducts **11** and **12** and the ester-linked mono-metronidazole mono-acid adducts **13a** and **13b**,[9] as growth inhibitors for the anaerobe *P. gingivalis*. In the process of developing a therapeutic agent for the inhibition of growth of *P. gingivalis*, the acquisition pathway for an essential growth requirement, haem **1**, was investigated. Comparison of the binding of these adducts to HA2 with haem **1** and the evaluation of their growth inhibitory activities against *P. gingivalis* provides a basis for discussing the potential of such porphyrin-based drugs as alternatives to metronidazole **4**.

Results and discussion

Design of an inhibitor

Two modes of targeting *P. gingivalis* are envisaged: disruption of the molecular recognition and porphyrin transport processes involving the HA2 receptors that are localised at the surface of the cell and "Trojan horse" delivery of adducts to confound the metabolic processing by the bacterium.[10]

Other organisms that transport haem do so by recognition of the central metal ion through chelation. This mode of recognition is evident in a model (Fig. 1a) derived from the X-ray crystal structure of *Serratia marcescens*, which has a typical haemophore for haem, the HasA receptor.[11] At the surface of the cell, the HA2 domain of *P. gingivalis* recognises porphyrin by a unique mechanism.[2,12] A model depicting this mode of recognition is shown in Fig. 1b.

Evidence from recent HA2 recognition studies, on a wide array of protoporphyrin and deuteroporphyrin isomers, has specified design facets for the synthesis of porphyrin-based growth inhibitors.[2] First, HA2 binds the porphyrin macrocycle without reference to the prosthetic metal centre in haemoglobin.[2] In order to harvest the advantage of this recognition selectivity, a modified free-base porphyrin macrocycle was chosen. This would render the porphyrin unpalatable to other microbial species, such as *Serratia marcescens*, where porphyrin transport involves recognition of the central metal.[11] Second, there is preliminary evidence that recognition by HA2 is dependent on the structure of the porphyrin macrocyle. At least one free propionic acid side-chain on the propionic (southern) aspect is necessary and certain modifications of the vinyl (northern) aspect of these haem analogues are not tolerated. Derivatisation of deuteroporphyrin IX (DPIX) **3** at positions 3 and 8 with sulfonic acid or ethylene glycol groups resulted in a prolonged lag phase and reduced rate of growth but an equal final biomass. Porphyrins with both propionic acid

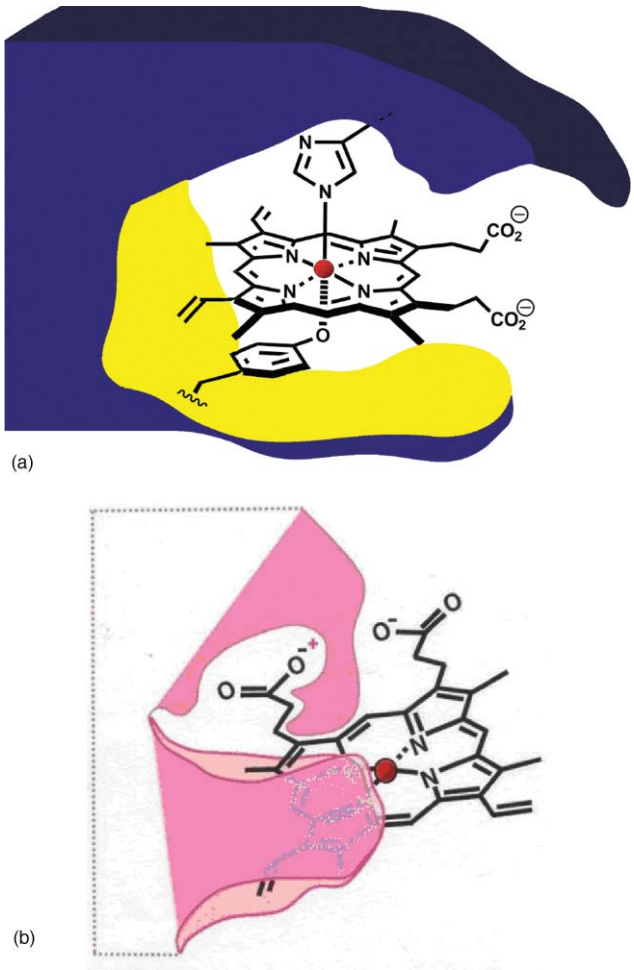

Fig. 1 Binding site for porphyrins (a) HasA from *Serratia marcescens*, (b) HA2 from *Porphyromonas gingivalis*.

side-chains derivatised as 2-hydroxyethyl esters could not support growth of cultures which corroborates that at least one free propionic acid group is crucial for recognition by HA2.[2]

Combining these two main design requirements led us to porphyrin–metronidazole conjugates as targets in which metronidazole is coupled to a porphyrin through a single propionic acid side-chain to form either a mono-amide, compounds **11** and **12**, or a mono-ester, compounds **13a** and **13b**. This ensures that one propionic acid is retained for HA2 recognition. DPIX **3** was chosen as it is recognised by HA2 and does not contain a central metal preventing its uptake by other bacteria. It has several advantages over haem **1** such as better water solubility and stability. Amide-linked porphyrin–antibiotic conjugates were utilised as well as the ester versions to overcome potential cleavage by esterases.

Synthesis

Deuterohaem was prepared from haem **1** in a resorcinol melt *via* the Schumm protiodevinylation reaction.[13] Demetallation of deuterohaem to yield DPIX **3** was achieved with iron powder Fe(0) in refluxing formic acid; these conditions give better results than the literature method[13] which uses Fe(0) in refluxing acetic acid. The metronidazole **4** derivative met-NH_2 **5** was prepared as

 This journal is © The Royal Society of Chemistry 2009

the di(hydrochloride) salt from **4** following the literature in 85% yield.[14]

Direct reaction of DPIX **3** and 1.1 equivalents of **5** using the peptide coupling reagent *O*-(benzotriazol-1-yl)-*N,N,N′,N′*-tetramethyluronium hexafluorophosphate (HBTU) was investigated. Only a very low yield of the mono-adducts **11** and **12** was obtained with the main product being the diamide **6**. The positive co-operativity seen in this reaction was unexpected, especially as Hayashi and his colleagues reported a negative co-operativity in diesterification of protoporphyrin that allowed isolation of protoporphyrin mono-*t*-butyl esters in high yield.[15]

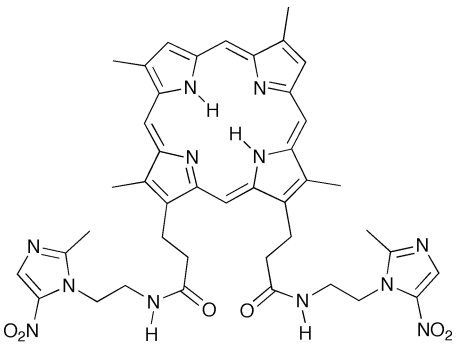

6

A second approach from DPIX **3** involved reacting 1.1 equivalents of **5** with the diacid chloride **7** derived from **3** and quenching the reaction with CH_3OH to give **9** and **10** in 27% yield along with the diamide **6** and DPIX dimethyl ester.

In order to obtain the required mono-adducts **9** and **10** in a higher yield, the peptide coupling method was utilised but a different strategy was adopted (Scheme 1). A mixture of isomers of mono-methyl mono-acid DPIX **8** was used as the starting material. Esters **8** were prepared by the controlled hydrolysis of DPIX dimethyl ester with 4 M hydrochloric acid.[16] With this strategy it is possible to use an excess of met-NH_2 **5**. The yield of **9** and **10** for reaction of **8** with **5** was increased to 88%.

Isolating the products as the methyl esters **9** and **10** rather than acids **11** and **12** allows for relatively easy chromatographic separation as it avoids the polar products. Isomers **9** and **10** were separated from the mixture by silica gel chromatography using a solvent gradient of 97 : 3 : 0.2 CH_2Cl_2–CH_3OH–$(CH_3CH_2)_3N$. This mixture was passed through a Zorbax Rx-SIL column eluting isocratically with a 99.5 : 0.5 : 0.2 mixture of CH_2Cl_2–CH_3OH–$(CH_3CH_2)_3N$ to separate the isomers. The fractions were re-chromatographed until sufficient purity was obtained as confirmed by analytical HPLC. 2D ^{1}H NMR studies described below were employed to identify the first fraction eluted as **9** and the second fraction as **10**. The methyl ester amide **9** was hydrolysed, in quantitative yield, to the corresponding free acid amide **11** by stirring in LiOH–CH_3OH–water at room temperature for 2 h. Similarly, methyl ester amide **10** was converted into the corresponding free acid amide **12** in quantitative yield.

The 2D ^{1}H NMR techniques COSY and NOESY were used for structure elucidation of the isomers **9** and **10** (Fig. 2). Spectra of **9** and **10** were fully assigned (see ESI† for full details). The key to assignment of these structures is to establish a connectivity between the metronidazole amine appendage and the propionyl side-chain to which it is attached. Identification of the elaborated

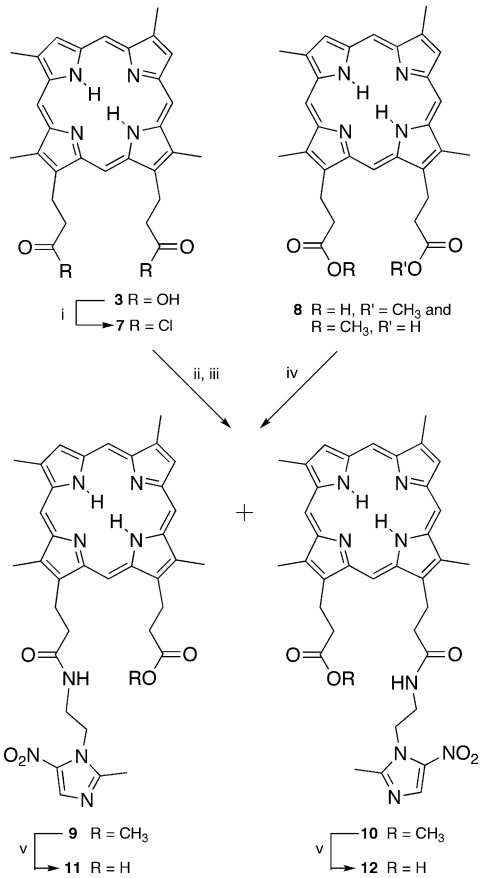

Scheme 1 *Reagents and conditions*: (i) thionyl chloride, reflux under N_2, 30 min; (ii) met-NH_2 **5** as diHCl salt, $(CH_3CH_2)_3N$, reflux under N_2, 3 h; (iii) CH_3OH; (iv) met-NH_2 **5** as diHCl salt, DIPEA and HBTU in CH_2Cl_2, stir under N_2,1 h; (v) LiOH–CH_3OH–water, stir, 2 h.

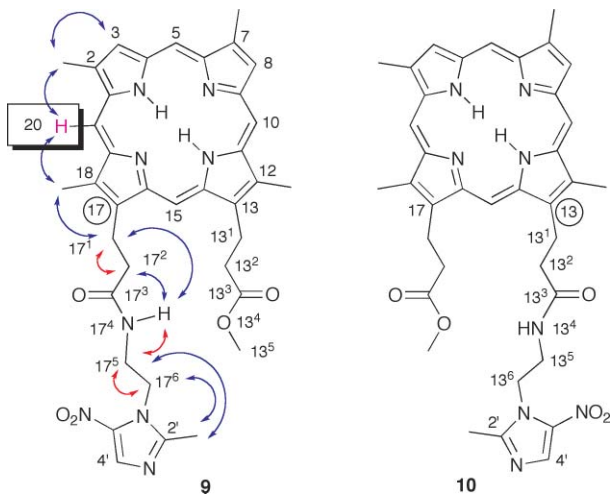

9 **10**

Fig. 2 Numbering system for **9** and **10** and key connectivities seen in the ^{1}H NMR NOESY (in blue) and COSY (in red) spectrum of **9**.

side-chain as being that at the 13-position or that at the 17-position completes the identification.

The protons of the metronidazole amine moiety could be readily identified. A broad triplet (δ 7.05) in the 1D ^{1}H NMR spectra of both isomers was attributed to –NH. This was found to couple, through 3-bond coupling, to a methylene at δ 3.49 (17^5 in the case

of **9** and 13[5] in the case of **10**). All other methylene protons are at least 4-bonds away. The COSY spectra allowed the visualisation of scalar couplings and readily established the adjacent methylene, that attached to the imidazole ring (17[6] in the case of **9** and 13[6] in the case of **10**). The NOESY spectra allowed the visualisation of vector couplings and showed connectivities between the imidazole 2′-methyl and each of these side-chain methylenes.

In order to determine which of the side-chains (13 or 17) bears the metronidazole appendage, a key starting point is to establish which of the four downfield singlets is attributable to the *meso*-proton at the 20-position. In spectra of **9**, there are four *meso*-proton resonances seen as singlets at δ 10.00, 10.06, 10.07, and 10.12; only the latter shows a NOESY coupling to two methyls (at δ 3.74 and 3.64) and hence it is assigned to the 20-H. The NOESY spectrum showed that the methyl resonating at δ 3.74 was adjacent to a β-pyrrolic proton (δ 9.10) and must be due to the methyl at the 2-position. The methyl (δ 3.64) is thus at the 18-position and it is coupled to the methylene 17^1 (δ 4.45) of the side-chain which is in turn coupled to the methylene 17^2 (δ 3.11). The resonances due to the methylenes 17^1 and 17^2 in the case of the first eluted fraction in the separation were found to exhibit NOESY coupling to the amide group proton and established this isomer as **9**. It was also possible to follow a path of connectivity down the other side of the molecule which showed that in the case of **9**, the 13-side-chain did not have the appended metronidazole appendage. Similarly consistent assignments were obtained from the analogous spectra of compound **10**, confirming this structure.

Metronidazole **4** was also attached to **3** by an ester linkage through one of the propionic acid side-chains of the porphyrin macrocycle. A stoichiometric amount of **4** was reacted with the diacid chloride **7** to yield the ester-linked mono-metronidazole mono-acid adducts **13a** and **13b**, the di-substituted version **14** and unreacted starting material **3** (Scheme 2).

Isomers **13a** and **13b** were separated from the mixture by silica gel chromatography using a 10 : 1 : 1 solvent gradient of CH_2Cl_2–CH_3OH–CH_3NO_2. The yield of **13a** and **13b** was 8%; attempts to improve this by increasing the quantity of **4** and lengthening the reaction time normally resulted in the formation of more di-substituted product **14**. The isomers **13a** and **13b** could not be separated by silica gel chromatography or high performance liquid chromatography (HPLC) employing a variety of solvents. A different approach to their separation was by functionalisation of the free propionic acid side-chain on **13a** and **13b** to accentuate the differences in the isomers and render them more chromatographically amenable. A series of ester protecting groups have been investigated for this purpose but separation of the isomers has not yet been accomplished. However, during this investigation, the isomers **13a** and **13b** were synthesised in 23% yield.

Binding studies

Binding studies were carried out as described previously[2] on various compounds to test their binding affinity to HA2. The results of these studies are presented in Fig. 3. Haem **1**, the mixture of **13a** and **13b**, the mixture of **11** and **12**, isomer 1 **11** and isomer 2 **12** all bind HA2 with a similar KD_{50} (15 ± 10 nM). This shows

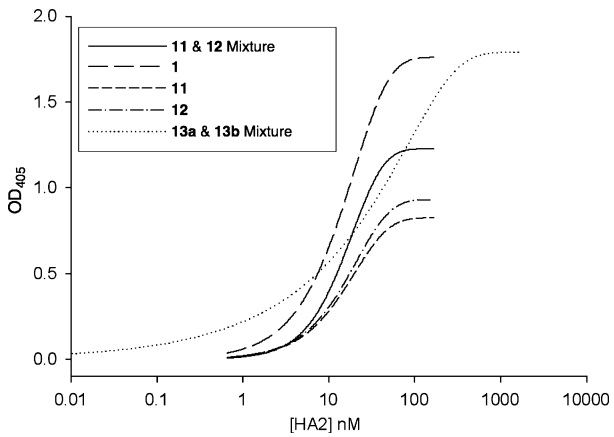

Fig. 3 The capacity of recombinant HA2 (rHA2) to bind porphyrin adducts was compared with haem **1** binding as measured by solid-phase ELISA.

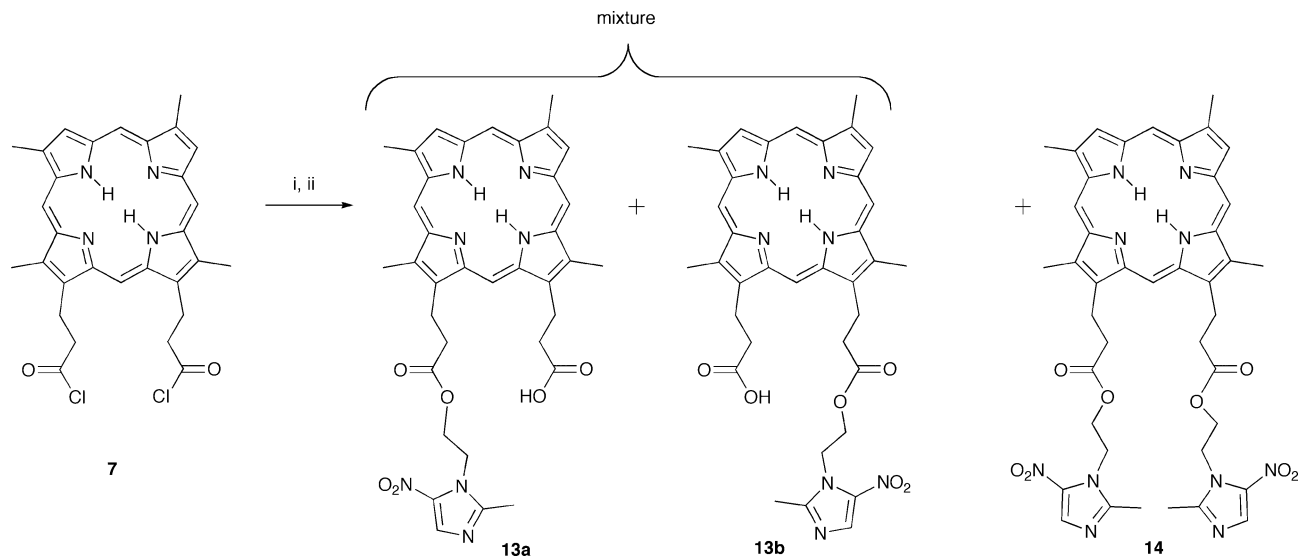

Scheme 2 *Reagents and conditions:* (i) metronidazole **4**, $(CH_3CH_2)_3N$, reflux under N_2, 1 h; (ii) water.

 This journal is © The Royal Society of Chemistry 2009

that HA2 binds all the compounds tested with high affinity. These results suggest that any response of *P. gingivalis* to the compounds tested in growth inhibition studies can be attributed to their uptake through recognition by HA2.

Growth inhibition studies

The conditions for growth of *P. gingivalis* were those previously described.[2] The following figures (Fig. 4 to 6) show the growth curves of *P. gingivalis* when administered with the tested compounds. Fig. 4a and b show growth curves of *P. gingivalis* for DPIX **3** and metronidazole **4**, respectively. As seen, there is no growth inhibition of *P. gingivalis* by **3** even at 20 μM. Instead **3** is a growth supplement for *P. gingivalis.* Fig. 4b shows complete inhibition of growth of *P. gingivalis* by **4** down to 2 μM and by 1 μM, **4** loses its activity after approximately 50 h followed by growth recovery of the *P. gingivalis* cells. The minimum inhibitory concentration (MIC) of **4** can be determined to be approximately 1 μM to 2 μM.

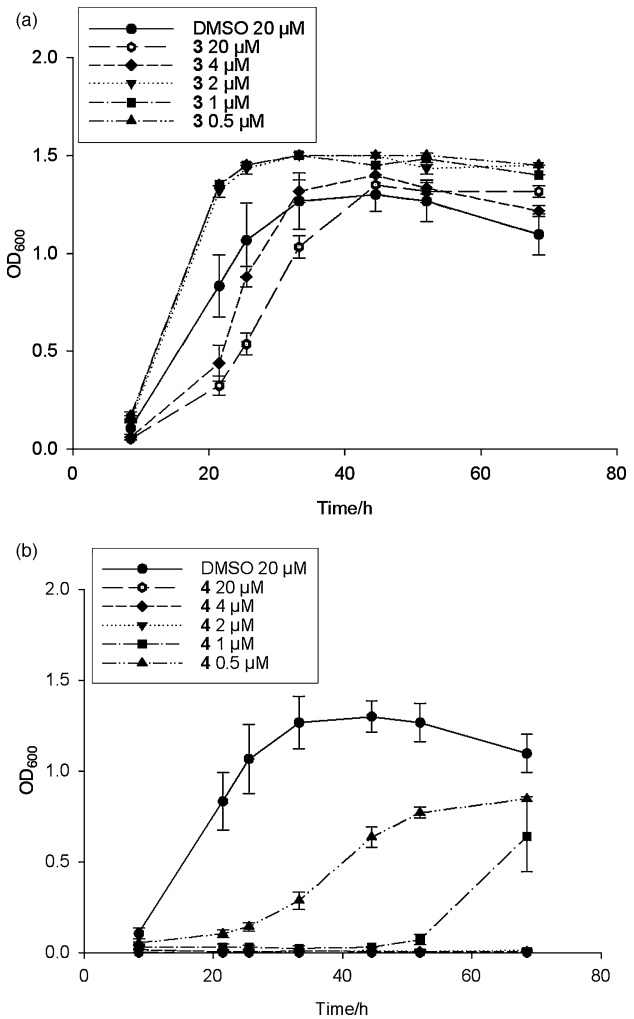

Fig. 4 *P. gingivalis* growth curves in response to (a) supplementation of DPIX **3** and (b) inhibition by metronidazole **4**.

Fig. 5 shows that there is poor inhibition of growth of *P. gingivalis* by the amide-linked mono-metronidazole mono-methyl ester adducts **9** and **10** even at 20 μM. There are two reasons

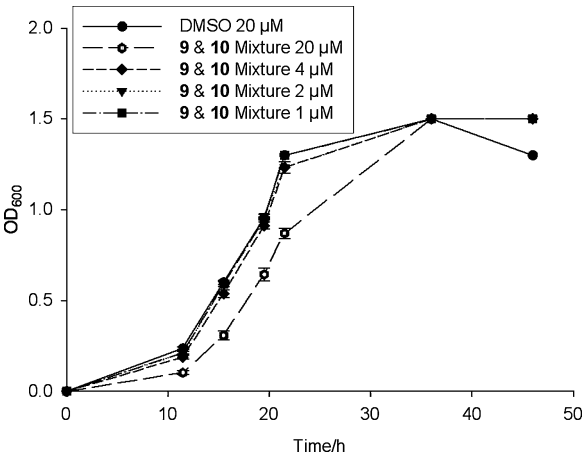

Fig. 5 *P. gingivalis* growth inhibition curves of amide esters **9** and **10**.

to explain this. Firstly, **9** and **10** lack the free propionic acid which rendered them poorly water-soluble. Secondly, binding studies using recombinant HA2 (rHA2) indicated binding of haem **1** to the HA2 domain by an interaction with the propionic acid groups of the haem **1** moiety and where esterification of the propionic acid groups eliminated recognition by rHA2.[2] Therefore, **9** and **10** could not be recognised by rHA2.

Metronidazole amine **5** is the putative product of cleavage of the adducts **11** and **12**. Fig. 6a shows complete inhibition of *P. gingivalis* growth at 20 μM and suppression of growth at 10 μM for about 55 h after which the *P. gingivalis* cells return to their original biomass. There is no effect on *P. gingivalis* at concentrations below 10 μM. MIC of **5** ranges from 10 μM to 20 μM.

The mixture **11** and **12** shows complete suppression of growth of *P. gingivalis* at 1.25 μM and suppression of growth at 0.65 μM for about 50 h, after which growth recovers (Fig. 6b). However, the *P. gingivalis* cells do not return to their original biomass and this suggests that there is still some suppression at 0.65 μM. MIC of the mixture of **11** and **12** ranges from 0.65 μM to 1.25 μM. Also, the ten- to twenty-fold gain of the adducts **11** and **12** over **5** suggests that there is porphyrin macrocycle recognition by HA2 which is crucial for the uptake of the antibiotic into the cell. However, further work is required to determine the actual mechanism of transport of **5** into the cell.

To address the effect of changing the positions of the protons on the vinyl face of the porphyrin macrocycle, the two isomers of the **11** and **12** mixture were separated. As the porphyrin ring is planar and the inner protons on N_2 are labile, there is pseudosymmetry in their structures (vertical two-fold axes in the plane of the porphyrin rings). Quinones are thought to be required as electron transport carriers for the later steps of anaerobic haem biosynthesis[17] and the supplementation of menadione may assist *P. gingivalis* in the metabolism and utilisation of these adducts. Therefore menadione was added as a supplement to the inoculant of *P. gingivalis.* The effect of varying the positions of the protons on the vinyl face of the porphyrin macrocycle on growth inhibition of *P. gingivalis* was evaluated. It was found that both **11** and **12** have equivalent potencies (MIC of 0.65 μM to 1.25 μM) against *P. gingivalis* (Fig. 6c and d).

This shows that changing the positions of the protons on the vinyl face of the porphyrin macrocycle does not affect the

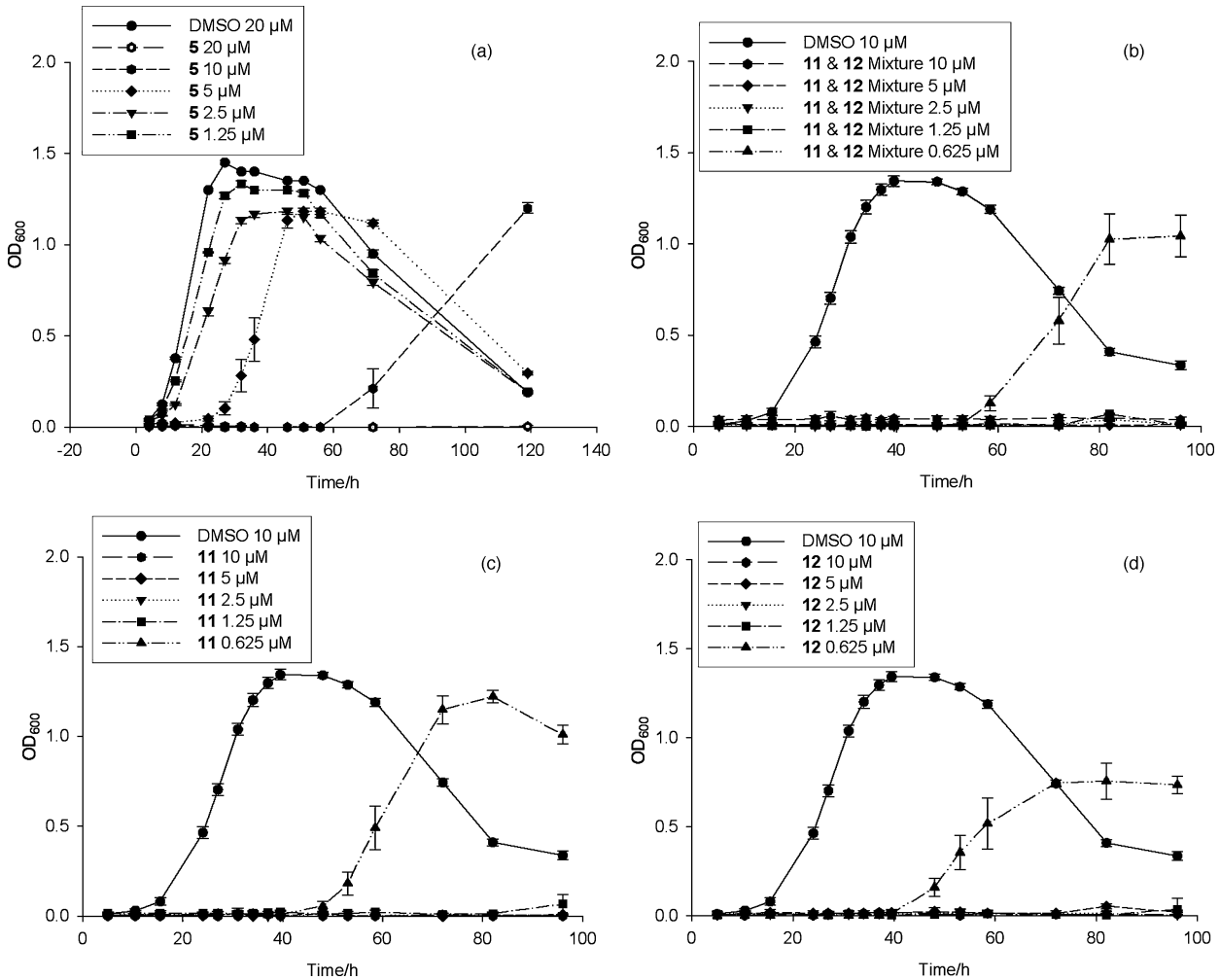

Fig. 6 *P. gingivalis* growth inhibition curves of (a) metronidazole amine **5**, (b) the mixture of **11** and **12**, (c) **11** and (d) **12**.

recognition by HA2, and supports the hypothesis of the structural requirements proposed for HA2 recognition. It should also be noted that there is no difference in growth inhibition between the **11** and **12** mixture and the resolved isomers **11** and **12**.

To investigate the selectivity of these promising porphyrin-linked nitroimidazole antibiotics, they were tested against other organisms and compared with the action of metronidazole **4** (Fig. 7).

Fig. 7a and b show the growth inhibitory activities of metronidazole **4** and the mixture of ester adducts **13a** and **13b** toward *P. gingivalis*, a related organism, *Prev. melaninogenica* and a non-related organism, *F. nucleatum.* Fig. 7a shows the growth inhibitory activity by **4** and it can be seen that there is complete indiscriminate suppression of all organisms by **4** at 20 μM and no recovery of the cells even after 68 h. Fig. 7b shows that there is only complete suppression of *P. gingivalis* with no recovery of the cells after 68 h at 20 μM by the mixture of **13a** and **13b**. The graph also shows that at the same concentration, there is no effect of the mixture of **13a** and **13b** on *Prev. melaninogenica* and only initial suppression of *F. nucleatum* although recovery of the *F. nucleatum* cells to their original biomass after 45 h indicates that the cells are not killed. This highlights the superior selectivity of the mixture of **13a** and **13b** towards *P. gingivalis* which was not achieved with **4**.

Conclusions

New porphyrin–metronidazole adducts were synthesised, the amide-linked adducts **11** and **12** and the ester-linked adducts **13a** and **13b**. Isomers **11** and **12** have not only been shown to be more potent than metronidazole **4** but there is also the potential for selective action against *P. gingivalis.* A ten- to twenty-fold gain of potency of the adducts **11** and **12** over metronidazole amine **5** suggests that there is porphyrin macrocycle recognition by HA2 which is crucial for the uptake of the antibiotic by the organism. Further work is required, however, to determine the actual mechanism of transport of the antibiotic into the cell. These adducts form the basis for the synthesis of a series of porphyrin-linked nitroimidazole adducts with the aspiration of creating a library of compounds for biological testing *in vitro* and eventually *in vivo.*

Experimental

General procedures

Melting points were recorded on a Gallenkamp melting point apparatus and are uncorrected. ^{1}H nuclear magnetic resonance

 This journal is © The Royal Society of Chemistry 2009

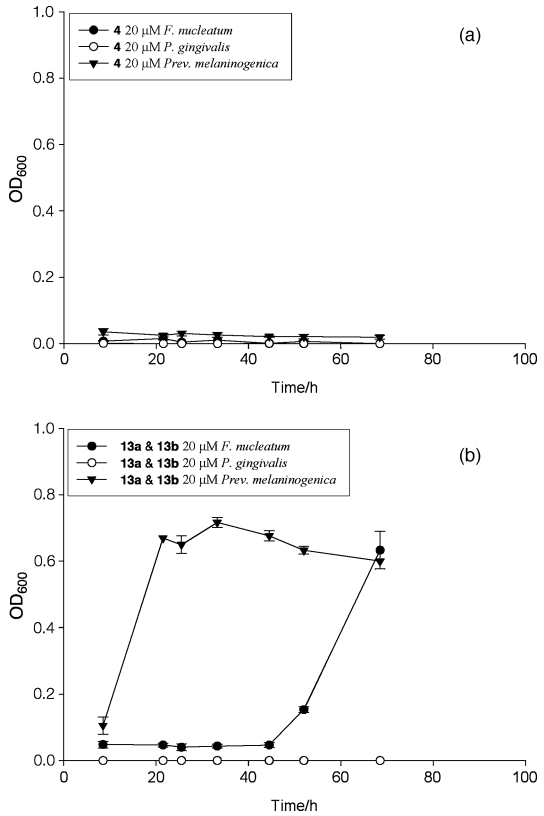

Fig. 7 Growth inhibitory activities of (a) metronidazole **4** and (b) the mixture of **13a** and **13b**.

(^{1}H NMR) spectra were recorded on a Bruker Avance DPX 200 spectrometer at a frequency of 200 MHz or a Bruker Avance DPX 300 spectrometer at a frequency of 300 MHz at 300 K. *J* values are given in Hz. MALDI-TOF mass spectra were recorded on a Micromass Tof Spec 2E spectrometer. Electrospray ionization (ESI) mass spectra were recorded on a ThermoQuest Finnigan LCQ Deca ion trap mass spectrometer. Infrared absorption spectra were recorded on a Shimadzu Model 8400 FTIR spectrophotometer and electronic absorption spectra were carried out on a Cary 5E UV-Vis spectrophotometer. Analytical thin layer chromatography (TLC) was performed using Merck Kieselgel silica gel 60 F-254 precoated sheets (0.2 mm) and preparative column chromatography was carried out routinely on Merck Kieselgel 60 silica gel (SiO_2, 0.040–0.063 mm). Analytical and preparative reverse phase HPLC was carried out on a Waters 600E solvent delivery system with a Rheodyne 7125 injector and a Waters 486 UV detector using the solvent system CH_2Cl_2–CH_3OH–$(CH_3CH_2)_3N$ (99.5 : 0.5 : 0.1).

DPIX amide-linked di-metronidazole adduct 6. DPIX **3** (40 mg, 0.078 mmol) was dissolved in DMF (2 cm^3) and CH_2Cl_2 (28 cm^3). To this was added **5** (22 mg, 0.090 mmol), *N,N′*-diisopropylethylamine (DIPEA, 0.03 cm^3, 0.125 mmol) and HBTU (34 mg, 0.090 mmol) and the mixture was stirred overnight at room temperature under N_2. The mixture was quenched with H_2O (80 cm^3), extracted into CH_2Cl_2 (3 × 60 cm^3), washed with H_2O, dried (anhydrous sodium sulfate) and filtered. The solvent was removed *in vacuo* to yield a black residue. The residue was purified by silica gel chromatography with an initial eluting solvent of CH_2Cl_2–CH_3OH (99 : 1). The polarity was increased to 98 : 2 upon which the main band eluted. The fractions that contained the main band were evaporated *in vacuo* to yield the di-metronidazole-substituted adduct **6** (29 mg, 56%) as a black solid. λ_{max} ($CHCl_3$) 400 (log ε dm^3 mol^{-1} cm^{-1} 4.59), 497 (3.49), 531 (3.28), 566 (3.19), 620 (2.97) nm; ν_{max} ($CHCl_3$) 3448 w (NH), 3024 m (aromatic CH), 2931 m (aliphatic CH), 1672 s (C=O), 1603/1465 m (C=C), 1531/1388 w (N=O) cm^{-1}; ^{1}H NMR (300 MHz; $CDCl_3$; $SiMe_4$) δ_H –4.73 (2H, s, inner NH), 1.97/1.99 (6H, s, N=C–*CH*$_3$), 2.93–3.00 (4H, m, –CH_2), 3.19–3.24 (4H, m, –CH_2), 3.40 (3H, s, –CH_3), 3.42 (3H, s, –CH_3), 3.55 (3H, s, –CH_3), 3.56 (3H, s, –CH_3), 3.90–3.96 (4H, m, –CH_2), 4.08–4.16 (4H, m, –CH_2), 7.58/7.60 (2H, s, NO_2C=*CH*), 7.75–7.79 (2H, br t, NH), 8.85 (2H, s, β-pyrrolic), 9.64 (1H, s, *meso* H), 9.68 (1H, s, *meso* H), 9.71 (1H, s, *meso* H), 9.76 (1H, s, *meso* H); *m/z* (ESI-MS) 815.3 [(M + H)$^+$ requires 815.9]; *m/z* (FTICR-MS) 815.3770 [(M + H)$^+$, calcd for [$C_{42}H_{46}N_{12}O_6$ + H$^+$]: 815.3736].

DPIX amide-linked mono-metronidazole mono-methyl adducts 9 and 10. Peptide coupling method. DPIX mono-methyl mono-acid **8** (60 mg, 0.114 mmol) was dissolved in CH_2Cl_2 (15 cm^3). To this was added **5** (168 mg, 0.691 mmol), *N,N′*-diisopropylethylamine (DIPEA, 0.2 cm^3, 0.830 mmol) and HBTU (264 mg, 0.696 mmol) and the mixture was stirred for 15 min at room temperature under N_2. The mixture was filtered and the products were separated by silica gel chromatography with **9** and **10** eluting with 97 : 3 CH_2Cl_2–CH_3OH (68 mg, 88%). **9/Fr 1:** ^{1}H NMR (300 MHz; $CDCl_3$) δ_H –3.93 (2H, s, inner NH), 2.30 (3H, s, N=C–*CH*$_3$), 3.11 (2H, t, *J* 7.6, –CH_2), 3.24 (2H, t, *J* 6.4, –CH_2), 3.33 (3H, s, –O*CH*$_3$), 3.49 (2H, m, –CH_2), 3.61 (3H, s, –CH_3), 3.64 (3H, s, –CH_3), 3.72 (3H, s, –CH_3), 3.74 (3H, s, –CH_3), 4.18 (2H, t, *J* 6.4, –CH_2), 4.35–4.40 (4H, m, –CH_2), 7.05 (1H, br s, O=C–*NH*), 8.47 (1H, s, NO_2C=*CH*), 9.08/9.10 (2H, s, β-pyrrolic H), 10.00 (1H, s, *meso* H), 10.06 (1H, s, *meso* H), 10.07 (1H, s, *meso* H), 10.12 (1H, s, *meso* H); *m/z* (ESI-MS) 677.5 [(M + H)$^+$ requires 677.7]. Retention time: 16.2 min; ZorbaxRx-SIL975.9; 1 mL min^{-1}. **10/Fr 2:** ^{1}H NMR (300 MHz; $CDCl_3$) δ_H –3.93 (2H, s, inner NH), 2.30 (3H, s, N=C–*CH*$_3$), 3.11 (2H, t, *J* 7.3, –CH_2), 3.24 (2H, t, *J* 6.8, –CH_2), 3.34 (3H, s, –O*CH*$_3$), 3.49 (2H, m, –CH_2), 3.61 (3H, s, –CH_3), 3.64 (3H, s, –CH_3), 3.72 (3H, s, –CH_3), 3.74 (3H, s, –CH_3), 4.18 (2H, t, *J* 6.8, –CH_2), 4.35–4.40 (4H, m, –CH_2), 7.05 (1H, br s, O=C–*NH*), 8.47 (1H, s, NO_2C=*CH*), 9.08/9.10 (2H, s, β-pyrrolic H), 10.00 (1H, s, *meso* H), 10.06 (1H, s, *meso* H), 10.07 (1H, s, *meso* H), 10.12 (1H, s, *meso* H); *m/z* (ESI-MS) 677.4 [(M + H)$^+$ requires 677.7]. Retention time: 17.6 min; ZorbaxRx-SIL975.9; 1 mL min^{-1}.

Acid chloride method. DPIX **3** (303 mg, 0.590 mmol) was refluxed in thionyl chloride (10 cm^3) under N_2 for 30 min. Upon cooling, excess thionyl chloride was removed *in vacuo.* The residue was dissolved in CH_2Cl_2 (50 cm^3) and met-NH_2 **5** (59 mg, 0.240 mmol) and $(CH_3CH_2)_3N$ (0.4 cm^3, 2.91 mmol) were added. The solution was refluxed under N_2 for 1 h and upon cooling the solvent was removed *in vacuo.* Toluene (20 cm^3) was added and evaporated *in vacuo.* A mixture of toluene (20 cm^3) and water (0.5 cm^3) was added and the two-phase mixture was stirred for 30 min. The solvent was removed *in vacuo* to yield a mixture of products as a black residue. This residue was purified by silica gel chromatography with an initial eluting solvent of CH_2Cl_2–CH_3OH–$(CH_3CH_2)_3N$ (99 : 1 : 0.2). The polarity was increased to

97 : 3 : 0.2 upon which a broad band containing **9** and **10** eluted. The fractions that contained the band were evaporated *in vacuo* to yield **9** and **10** as a black residue (108 mg, 27%).

Separation of DPIX amide-linked mono-metronidazole mono-acid adducts 9 and 10. The residue of **9** and **10** from method 2 (108 mg) was re-dissolved in a small amount of CH_2Cl_2 and passed through a Zorbax Rx-SIL column eluting isocratically with CH_2Cl_2–CH_3OH–$(CH_3CH_2)_3N$ (99.5 : 0.5 : 0.2) to resolve the two isomers **9** and **10**. The fractions were re-chromatographed 12 times until sufficient purity was obtained as confirmed by analytical HPLC.

DPIX amide-linked mono-metronidazole mono-acid adducts 11 and 12. Method 1. Hydrolysis of the combined isomers **9** and **10** (68 mg, 0.101 mmol) occurred with LiOH (222 mg, 9.30 mmol) in CH_3OH–THF–H_2O (3 : 4 : 1) with stirring for 2 h to give **11** and **12** (67 mg, quant.). λ_{max} ($CHCl_3$) 399 (log ε dm^3 mol^{-1} cm^{-1} 4.55), 496 (3.72), 531 (3.60), 565 (3.54), 621 (3.45) nm; ν_{max} (KBr) 3493 w (NH), 3068 m (OH), 2980 m (aromatic CH), 2855 m (aliphatic CH), 1710 s (C=O), 1650/1467 m (C=C), 1536/1364 w (N=O), 1150 m (C–O) cm^{-1}; ^{1}H NMR (300 MHz; DMSO-d_6) δ_H −4.09 (2H, s, inner NH), 2.36 (3H, s, N=C–*CH*$_3$), 2.95–2.97 (4H, m, –CH_2), 3.48–3.50 (2H, m, –CH_2), 3.57–3.74 (12H, m, –CH_3), 4.14–4.17 (2H, br t, –CH_2), 4.30–4.32 (4H, m, –CH_2), 7.98 (1H, s, NO_2C=*CH*), 9.27 (2H, s, β-pyrrolic), 9.70 (1H, br s, OH), 10.21–10.27 (4H, m, *meso* H), 10.54 (1H, s, NH); *m/z* (ESI-MS) 663.5 [(M + H)$^+$ requires 663.7]; *m/z* (FTICR-MS) 663.3012 [(M + H)$^+$, calcd for [$C_{36}H_{38}N_8O_5$ + H$^+$]: 663.3038]. **Method 2.** Separated isomer residues **9** (5 mg, 0.007 mmol) and **10** (5 mg, 0.007 mmol) were re-dissolved in CH_2Cl_2 (2 cm^3), then a solution of NaOH (2 M, 0.8 cm^3), CH_3OH (4 cm^3) and dioxane (2 cm^3) was added. The mixture was stirred for 9 h at room temperature. The mixture was acidified to approximately pH 3 with a solution of hydrochloric acid (2 M) and extracted into CH_2Cl_2 (3 × 10 cm^3). The combined organic extracts were washed with water (2 × 10 cm^3), brine (1 × 10 cm^3), dried (anhydrous sodium sulfate) and the solvent removed *in vacuo* to yield **11** (5 mg, quant.) and **12** (5 mg, quant.) as black residues. **11/Fr 1:** ^{1}H NMR (200 MHz; DMSO-d_6) δ_H −3.97 (2H, s, inner NH), 2.17 (3H, s, N=C–*CH*$_3$), 3.05 (2H, t, *J* 4.8, –CH_2), 3.28 (2H, t, *J* 4.8, –CH_2), 3.44 (2H, t, *J* 3.9, –CH_2), 3.69 (3H, s, –CH_3), 3.70 (3H, s, –CH_3), 3.79 (3H, s, –CH_3), 3.83 (3H, s, –CH_3), 4.24 (2H, t, *J* 3.9, –CH_2), 4.36 (2H, t, *J* 4.9, –CH_2), 4.44 (2H, t, *J* 4.9, –CH_2), 8.00 (1H, s, NO_2C=*CH*), 8.29 (1H, br s, O=C–*NH*), 9.38/9.40 (2H, s, β-pyrrolic H), 10.35–10.39 (4H, m, *meso* H), 12.35 (1H, br s, O=C–*OH*). **12/Fr 2:** ^{1}H NMR (200 MHz; DMSO-d_6) δ_H −3.98 (2H, s, inner NH), 2.14 (3H, s, N=C–*CH*$_3$), 3.06 (2H, t, *J* 6.9, –CH_2), 3.29 (2H, t, *J* 6.9, –CH_2), 3.36 (2H, t, *J* 5.7, –CH_2), 3.66 (3H, s, –CH_3), 3.72 (3H, s, –CH_3), 3.78 (3H, s, –CH_3), 3.82 (3H, s, –CH_3), 4.23 (2H, t, *J* 5.7, –CH_2), 4.35 (2H, t, *J* 6.8, –CH_2), 4.45 (2H, t, *J* 6.8, –CH_2), 7.99 (1H, s, NO_2C=*CH*), 8.26 (1H, br s, O=C–*NH*), 9.38/9.40 (2H, s, β-pyrrolic H), 10.34–10.38 (4H, m, *meso* H), 12.35 (1H, br s, O=C–*OH*).

DPIX ester-linked mono-metronidazole mono-acid adducts 13a and 13b and DPIX ester-linked di-metronidazole adduct 14. DPIX **3** (200 mg, 0.392 mmol) was converted to **7** as above. The product was dissolved in CH_2Cl_2 (50 cm^3) and metronidazole **4** (27 mg, 0.157 mmol) and $(CH_3CH_2)_3N$ (5 drops) were added. The solution was refluxed under N_2 for 1 h and upon cooling the solvent was removed *in vacuo.* Toluene (20 cm^3) was added and evaporated *in vacuo.* A mixture of toluene (20 cm^3) and water (0.5 cm^3) was added and the two-phase mixture was stirred for 30 min. The solvent was removed *in vacuo* to yield a mixture of products as a black residue. The residue was purified by silica gel chromatography with an initial eluting solvent of CH_2Cl_2–CH_3OH–CH_3NO_2 (30 : 1 : 1). The polarity was increased to 20 : 1 : 1 upon which the first band eluted. The polarity was further increased to 10 : 1 : 1 upon which the second band eluted. The fractions that contained the first band were evaporated *in vacuo* to yield the di-metronidazole-substituted adduct **14** (12 mg, 4%) as a black solid. λ_{max} ($CHCl_3$) 400 (log ε dm^3 mol^{-1} cm^{-1} 5.10), 497 (3.99), 530 (3.72), 566 (3.63) and 620 (3.40) nm; ν_{max} ($CHCl_3$) 3316 w (NH), 2992 m (aromatic CH), 2900 m (aliphatic CH), 1737 s (C=O), 1661/1465 m (C=C), 1528/1364 w (N=O), 1220 m (C–O) cm^{-1}; ^{1}H NMR (300 MHz; $CDCl_3$; $SiMe_4$) δ_H −4.04 (2H, s, inner NH), 1.54 (3H, s, N=C–*CH*$_3$), 1.56 (3H, s, N=C–*CH*$_3$), 3.17 (4H, t, *J* 7.4, –CH_2), 3.56/3.57 (6H, s, –CH_3), 3.70/3.72 (6H, s, –CH_3), 3.77–3.86 (4H, m, –CH_2), 4.07–4.14 (4H, m, –CH_2), 4.32 (4H, t, *J* 7.4, –CH_2), 7.42 (1H, s, NO_2C=*CH*), 7.47 (1H, s, NO_2C=*CH*), 9.05 (2H, s, β-pyrrolic H), 9.91 (1H, s, *meso* H), 9.96 (1H, s, *meso* H), 10.03 (1H, s, *meso* H), 10.15 (1H, s, *meso* H); *m/z* (MALDI-TOF) 817.7 [(M + H)$^+$ requires 817.9]; *m/z* (FTICR-MS) 817.3349; [(M + H)$^+$, calcd for [$C_{42}H_{44}N_{10}O_8$ + H$^+$]: 817.3416]. The fractions that contained the second band were evaporated *in vacuo* to yield **13a** and **13b** (26 mg, 8%) as a black solid. λ_{max} ($CHCl_3$) 399 (log ε dm^3 mol^{-1} cm^{-1} 5.11), 497 (3.99), 530 (3.70), 566 (3.59) and 620 (3.36) nm; ν_{max} ($CHCl_3$) 3694 m (NH), 3581 m (OH), 3089 m (aromatic CH), 2927 m (aliphatic CH), 1730 s (C=O), 1602/1467m (C=C), 1520/1364 w (N=O), 1220 m (C–O) cm^{-1}; ^{1}H NMR (300 MHz; $CDCl_3$; $SiMe_4$) δ_H −4.32 (2H, s, inner NH), 0.78 (3H, s, N=C–*CH*$_3$), 3.09–3.15 (2H, br t, –CH_2), 3.23–3.27 (2H, br t, –CH_2), 3.43–3.65 (12H, m, –CH_3), 3.90–3.97 (4H, m, –CH_2), 4.04–4.21 (4H, m, –CH_2), 7.11 (1H, s, NO_2C=*CH*), 8.92/8.96 (2H, s, β-pyrrolic H), 9.81–9.91 (4H, m, *meso* H); *m/z* (MALDI-TOF) 664.5 [(M + H)$^+$ requires 664.7]; *m/z* (FTICR-MS) 664.2869 [(M + H)$^+$, calcd for [$C_{36}H_{37}N_7O_6$ + H$^+$]: 664.2879].

DPIX ester-linked mono-metronidazole mono-acid adducts 13a and 13b. DPIX **3** (50 mg, 0.098 mmol) was dissolved in refluxing thionyl chloride (10 cm^3) under N_2 and reacted for 45 min. The mixture was cooled and excess thionyl chloride was removed *in vacuo.* The residue was dissolved in CH_2Cl_2 (50 cm^3) and **4** (7 mg, 0.041 mmol) and $(CH_3CH_2)_3N$ (0.07 cm^3, 0.501 mmol) were added. The solution was refluxed under N_2 for 3 h and allowed to cool. DMF (0.03 cm^3), dimethyl-*tert*-butylsilyl chloride (18 mg, 0.119 mmol) and imidazole (16 mg, 0.235) were added and the mixture was stirred for 14 h. The solvent was removed *in vacuo* to yield a mixture of products as a black residue. The residue was purified by silica gel chromatography with the eluting solvent of **13a** and **13b** (15 mg, 23%) being CH_2Cl_2–CH_3OH (10 : 1).

General procedures for biological testing. The translated product of a synthetic HA2 gene, derived from the sequence of RgpA, was expressed in *E. coli* with a C-terminal polyhistidine tag,[18] was functionally purified by Hb-agarose affinity chromatography as previously described and is referred to as rHA2.

 This journal is © The Royal Society of Chemistry 2009

When analysed under reducing conditions by SDS-PAGE, rHA2 runs anomalously as a single band (estimated >98% purity) at 19 kDa.[18] Porphyrin adducts were used to coat ELISA plates as described previously[2] and binding of rHA2 was detected using anti-gingipain monoclonal antibody (mAb) 5A1.[19] Secondary goat anti-mouse antibody conjugated with alkaline phosphatase (AP) was supplied by Dako Corporation. 4-Nitrophenylphosphate (*p*-NPP) was supplied by Boehringer. *P. gingivalis* ATCC 33277 was used in all growth assays and cultures were anaerobically grown at 37 °C in an atmosphere containing CO_2 (5%), H_2 (10%) and N_2 (85%). *P. gingivalis* was cultured in CDC broth supplemented with menadione and haem **1**.[2] For experimental evaluation, log phase cultures were passaged as a 1% inoculum into CDC medium supplemented with menadione only. Under this condition the cells had sufficient haem **1** reserves to grow through a complete cycle as reported previously.[2] The growth of the *P. gingivalis* cells in triplicate cultures was monitored over 5 days (120 h) and growth was noted by the turbidity of the medium and recorded as the optical density at 600 nm against reagent blanks. Data show mean values and standard errors. Porphyrins, adducts and metronidazole derivatives were prepared as 10 mM stock solutions in DMSO [Merck] and diluted into CDC media. To control the possible inhibition of *P. gingivalis* by DMSO, all cultures were adjusted to contain levels of this solvent equivalent to the highest concentration used in the experiment. In this study, the choice of porphyrins was limited to those that were stable and soluble (or at least sparingly soluble) in water. All biological testing results were representative of at least three experiments.

Acknowledgements

This work was supported by grants from the Australian Research Council and The University of Sydney.

References

1 J. M. Roper, E. Raux, A. A. Brindley, H. L. Schubert, S. E. Gharbia, H. N. Shah and M. J. Warren, *J. Biol. Chem.*, 2000, **275**, 40316–40323.
2 M. Paramaesvaran, K.-A. Nguyen, E. Caldon, J. A. McDonald, S. Najdi, G. Gonzaga, D. B. Langley, A. A. Decarlo, M. J. Crossley, N. Hunter and C. A. Collyer, *J. Bacteriol.*, 2003, **185**, 2528–2537.
3 R. J. Gibbons and J. B. Macdonald, *J. Bacteriol.*, 1960, **80**, 164–170.
4 B. C. Lee, *Mol. Microbiol.*, 1995, **18**, 383–390.
5 P. P. Poulet, D. Duffaut and J. Ph. Lodter, *J. Clin. Periodontol.*, 1999, **26**, 261–263.
6 A. B. Novaes Jr., M. D. Uzeda, M. E. F. Fonseca and A. C. R. Feitosa, *J. Antimicrob. Chemother.*, 1991, **28**, 151–154.
7 B. J. Paster, S. K. Boches, J. L. Galvin, R. E. Ericson, C. N. Lau, V. A. Levanos, A. Sahasrabudhe and F. E. Dewhirst, *J. Bacteriol.*, 2001, **183**, 3770–3783.
8 I. Stojiljkovic, V. Kumar and N. Srinivasan, *Mol. Microbiol.*, 1999, **31**, 429–442.
9 M. Crossley, P. Thordarson, N. Hunter, B. Yap and C. A. Collyer, *PCT Int. Appl.*, WO 2006005137, A1 20060119, 2006.
10 N. Hunter, M. J. Crossley, B. C.-M. Yap and C. A. Collyer, *Australian Microbiol.*, 2005, **27**, 122–123.
11 X. P. Arnoux, R. Haser, N. Izadi, A. Lecroisey, M. Delepierre, C. Wandersman and M. Czjek, *Nat. Struct. Biol.*, 1999, **7**, 516–520.
12 N. Hunter, K.-A. Nguyen, J. A. McDonald, M. J. Quinn, D. B. Langley, M. J. Crossley and C. A. Collyer, *J. Porphyrins Phthalocyanines*, 2002, **6**, 774–782.
13 K. M. Smith, *Porphyrins and Metalloporphyrins*, Elsevier Scientific Publishing Company, Amsterdam, 1976.
14 M. P. Hay, W. R. Wilson, J. W. Moselen, B. D. Palmer and W. A. Denny, *J. Med. Chem.*, 1994, **37**, 381–391.
15 T. Matsuo, T. Hayashi and Y. Hisaeda, *J. Am. Chem. Soc.*, 2002, **124**, 11234–11235.
16 S. M. Sondhi, A. Magan and J. W. Lown, *Bull. Chem. Soc. Jpn.*, 1992, **65**, 579–585.
17 J. M. Jacobs and N. J. Jacobs, *Biochem. Biophys. Res. Commun.*, 1977, **78**, 429–433.
18 D. B. Langley, C. A. Collyer and N. Hunter, *PCT Int. Appl.*, WO 2002061091, 2002.
19 A. A. DeCarlo, M. Paramaesvaran, P. L. Yun, C. A. Collyer and N. Hunter, *J. Bacteriol.*, 1999, **181**, 3784–3791.